

High-energy magnetic excitations from dynamic stripes in $\text{La}_{1.875}\text{Ba}_{0.125}\text{CuO}_4$

Guangyong Xu,¹ J. M. Tranquada,¹ T. G. Perring,² G. D. Gu,¹ M. Fujita,³ and K. Yamada³

¹*Condensed Matter Physics & Materials Science Department,
Brookhaven National Laboratory, Upton, New York 11973, USA*

²*ISIS Facility, Rutherford Appleton Laboratory, Chilton, Didcot, Oxon, OX11 0Qx, UK*

³*Institute for Materials Research, Tohoku University, Sendai, 980-8577, Japan*

(Dated: April 5, 2018)

We use inelastic neutron scattering to study the temperature dependence of magnetic excitations (for energies up to 100 meV) in the cuprate $\text{La}_{1.875}\text{Ba}_{0.125}\text{CuO}_4$. This compound exhibits stripe order below a temperature of ~ 50 K; previous measurements have shown that the magnetic excitations of the stripe-ordered phase have an hour-glass-like dispersion, with a saddle point at ~ 50 meV. Here we compare measurements in the disordered phase taken at 65 and 300 K. At energies on the scale of $k_{\text{B}}T$, there is substantial momentum-broadening of the signal, and the low-energy incommensurate features can no longer be resolved at 300 K. In contrast, there is remarkably little change in the scattered signal for energies greater than $k_{\text{B}}T$. In fact, the momentum-integrated dynamic susceptibility is almost constant with temperature. We suggest that the continuity of higher-energy magnetic excitations is strong evidence for dynamic stripes in the high-temperature, disordered phase. We reconsider the nature of the magnetic dispersion, and we discuss the correspondences between the thermal evolution of magnetic stripe correlations with other electronic properties of the cuprates.

PACS numbers: 74.72.Dn, 74.81.2g, 75.40.Gb, 78.70.Nx

I. INTRODUCTION

Antiferromagnetic interactions are commonly believed to play a crucial role in the mechanism of high-temperature superconductivity in the cuprates.^{1,2} While the long-range Néel order of the insulating parent compounds is suppressed when a small density of holes is doped into the planes, dynamic spin correlations nevertheless persist into the superconducting phase. A central debate concerns the origin of the magnetic excitations. They have been attributed both to remnants of the parent insulator due to segregation of the doped holes into “stripes”^{3,4,5,6} and, alternatively, to excitations of the charge carriers across the Fermi surface, with enhancements due to electronic interactions.^{7,8,9,10,11}

Recent inelastic neutron scattering studies have made it clear that the magnetic excitations from various cuprate families, such as $\text{La}_{2-x}\text{Sr}_x\text{CuO}_4$ (LSCO)^{12,13,14,15,16,17} and $\text{YBa}_2\text{Cu}_3\text{O}_{6+x}$ (YBCO),^{18,19,20,21,22} share similar traits. Many of the observed features can be described with a phenomenological model involving a universal magnetic excitation spectrum multiplied by a spin-gap function.²³ The onset of the spin gap below the superconducting transition temperature, T_c , together with the shift in spectral weight from below to above the gap, can qualitatively reproduce the commensurate “resonance” peak observed in YBCO^{24,25} and $\text{Bi}_2\text{Sr}_2\text{CaCu}_2\text{O}_{8+\delta}$ (BSCCO),²⁶ and the incommensurate resonance in LSCO,^{12,14,16} when these systems go into the superconducting state. The magnitude of the spin gap is material dependent and correlated with T_c .²⁷ Given these universal trends, it is reasonable to anticipate that the electronic correlations underlying the magnetic response

must be common to the various cuprate families.

The sample studied here, $\text{La}_{1.875}\text{Ba}_{0.125}\text{CuO}_4$ [LBCO ($x = 1/8$)], is a compound in which superconductivity is anomalously suppressed ($T_c < 6$ K for our sample²⁸) by spin and charge stripe ordering. The existence of static spin and charge stripes at temperatures below the structural transition at $T_{\text{st}} \sim 54$ K has been confirmed by neutron,²⁹ resonant soft-X-ray,³⁰ and hard-X-ray³¹ diffraction measurements. Further evidence of the spin order (below 40 K) comes from magnetization³² and muon spin-rotation³³ studies. The high-energy excitation spectrum from LBCO ($x = 1/8$) in the stripe ordered state has been established in our previous experiment.²⁸ Unlike the isostructural nickelate compound $\text{La}_{2-x}\text{Sr}_x\text{NiO}_4$, where spin-wave-like excitations are observed in association with diagonal stripe order,^{34,35,36} the magnetic spectrum from our sample is very similar to that observed in other high- T_c cuprates,^{16,18,19,20} where static stripes are absent. The spectrum was found to disperse only inwards from the incommensurate elastic peaks, and to merge at the antiferromagnetic wave vector at an energy of ~ 50 meV. Above this saddle-point energy, the excitations disperse outward from the commensurate position again, but with an apparent 45° rotation of the anisotropic intensity pattern for wave vectors in the a - b plane, compared to the pattern at energies below the saddle point.

The fact that LBCO ($x = 1/8$) exhibits a stripe-ordered phase makes it an exception compared to the other cuprates studied so far, in the sense that there is little ambiguity on the origin of the incommensurate magnetic response. Consequently, the remarkable similarities of the magnetic excitations among these various systems suggest that stripe correlations represent a prime candi-

date for explaining the universal behavior. Of course, if the concept of dynamic stripes is to be taken seriously, it is important to fully characterize the magnetic excitations of a system where a good case for dynamic stripes can be made. A previous study²⁹ of LBCO ($x = 1/8$) focused on low-energy excitations (≤ 12 meV) and demonstrated a continuous evolution of the magnetic correlations across T_{st} , consistent with a transition from static to dynamic stripes.

Here we present an investigation of the high-energy magnetic excitations (up to ~ 100 meV) in LBCO ($x = 1/8$) at several different temperatures using a time-of-flight neutron spectrometer. In particular, we compare measurements at 65 K and 300 K, where there is no stripe order, with those in the ordered phase at 10 K. A thermal broadening of the momentum (\mathbf{Q}) dependence and reduction of the incommensurability is observed with increasing temperature in the low-energy part of the spectrum ($\lesssim 20$ meV), consistent with previous work²⁹; however, the excitations near and above the saddle-point energy (~ 50 meV) show remarkably little change. After describing the experimental details in Sec. II and presenting the results in Sec. III, we will argue in Sec. IV that they provide strong evidence for, and a signature of, dynamic stripes. We will discuss the relationship between the thermal evolution of the spin fluctuations and other electronic properties of the cuprates.

II. EXPERIMENT

Our sample consists of four single crystals of LBCO ($x = 1/8$) with total mass of 58 g; these are the same crystals used in Ref. 28. The crystals were grown by the traveling-solvent floating-zone method at Brookhaven National Laboratory. At room temperature, LBCO ($x = 1/8$) is in the high-temperature-tetragonal (HTT) phase (space group $I4/mmm$); it transforms to the low-temperature-orthorhombic (LTO) phase (space group $Bmab$) at ~ 235 K, and to the low-temperature-tetragonal (LTT) phase (space group $P4_2/ncm$) at $T_{\text{st}} \approx 54$ K (Ref. 32). As the small changes in lattice parameters are well below the resolution of the present measurements, we will use the high-temperature-tetragonal unit cell, with $a = b = 3.78$ Å and $c = 13.2$ Å, to describe our results. The crystals are co-aligned together so that the effective mosaic is $\lesssim 1^\circ$ in the a - c plane and $\lesssim 2^\circ$ in the b - c plane.

T_c , measured with magnetic susceptibility on pieces cut from the ends of our crystals, is generally less than 6 K. Other characterizations have recently been performed on sister crystals. Measurements³⁷ of the in-plane resistivity and optical conductivity for $T > T_{\text{st}}$ are quantitatively similar to results for LSCO at the same hole concentration. For $T < T_{\text{st}}$, the optical conductivity, and also angle-resolved photoemission spectra,³⁸ provide evidence for a d -wave-like gap.

Inelastic neutron scattering experiments have been

performed on the MAPS time-of-flight spectrometer at the ISIS facility, Rutherford Appleton Laboratory. For all measurements, the c -axis was oriented parallel to the incident neutron beam. Data were collected with incident energies of $E_i = 80$ meV and 140 meV (and chopper frequencies of 300 Hz and 400 Hz, respectively). For the data presented here, we have taken advantage of the four-fold crystalline symmetry to combine data from four equivalent Brillouin zones (all at the same $|\mathbf{Q}|$) into one, thus improving the statistics. The scattered intensity has been converted to absolute units by normalization to measurements of diffuse scattering from a vanadium sample.

The differential scattering cross section can be written as

$$\frac{d\sigma}{d\Omega_f dE_f} = \frac{k_f}{k_i} \tilde{S}(\mathbf{Q}, \omega), \quad (1)$$

where $\tilde{S}(\mathbf{Q}, \omega)$ is the dynamic structure factor, with units of mbarn/(steradian meV formula unit), and k_i and k_f are the initial and final neutron wave vectors. For magnetic correlations, one has

$$\tilde{S}(\mathbf{Q}, \omega) = \left(\frac{\gamma r_0}{2}\right)^2 f^2(\mathbf{Q}) S(\mathbf{Q}, \omega), \quad (2)$$

where $f(\mathbf{Q})$ is the magnetic form factor for Cu^{2+} , $S(\mathbf{Q}, \omega)$ is the Fourier transform of the spin-spin correlation function, and $(\gamma r_0/2)^2 = 72.6$ mbarn. The function $S(\mathbf{Q}, \omega)$ is related to the imaginary part of the dynamical susceptibility by the formula

$$S(\mathbf{Q}, \omega) = \chi''(\mathbf{Q}, \omega) / \left(1 - e^{-\hbar\omega/k_B T}\right). \quad (3)$$

The magnetic form factor for Cu^{2+} is known to be anisotropic,³⁹ falling off more slowly for \mathbf{Q}_\perp , perpendicular to the CuO_2 planes, than for \mathbf{Q}_\parallel . For the chosen sample orientation ($\mathbf{c} \parallel \mathbf{k}_i$), we can collect data as a function of \mathbf{Q}_\parallel and $\hbar\omega$; however, the value of \mathbf{Q}_\perp varies with \mathbf{Q}_\parallel and $\hbar\omega$, and it also depends on E_i . We have taken into account all three components of \mathbf{Q} when correcting for the magnetic form factor to obtain S and χ'' .

III. RESULTS AND ANALYSIS

Figure 1 shows constant-energy slices of the scattering near the antiferromagnetic wave vector, $\mathbf{Q}_{\text{AF}} = (0.5, 0.5)$, for three temperatures. The energy increases (6, 41, and 95 meV) from bottom to top, and the temperature increases (10, 65, and 300 K) from left to right. The intensity peaked near \mathbf{Q}_{AF} we attribute to magnetic scattering; the “background” signal is due mostly to phonons. The bright diagonal stripe of scattering in the upper-right corner of the panels for 41 meV is also attributed to phonons.

The incommensurate peaks characteristic of stripe correlations^{29,40} are clearly seen in the $\hbar\omega = 6$ meV data

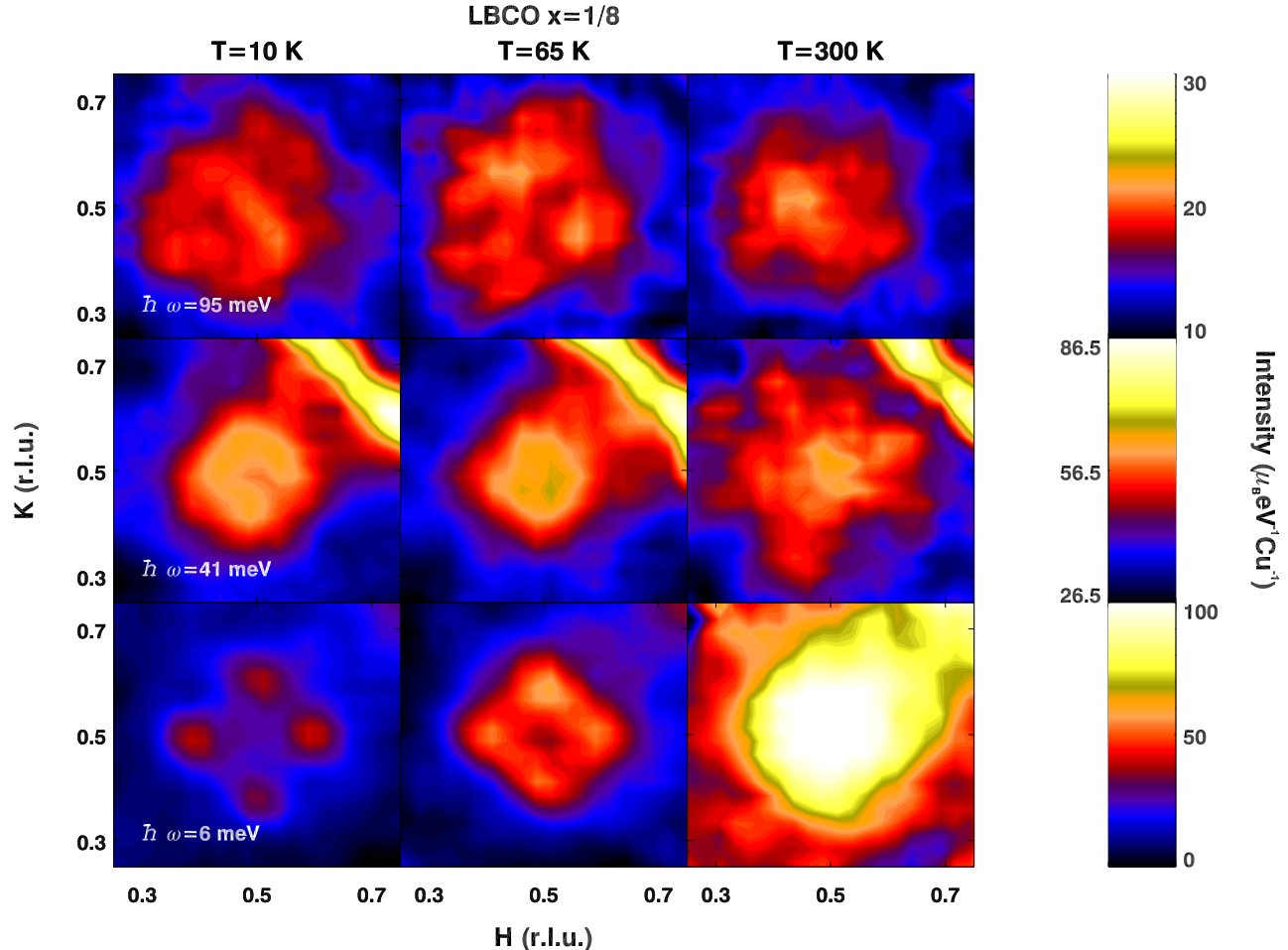


FIG. 1: (Color online) Constant energy cuts around $\mathbf{Q}_{\text{AF}} = (0.5, 0.5)$ from data taken on MAPS at different temperatures. The bottom and middle rows are data taken with $E_i = 80$ meV, and the top row are data taken with $E_i = 140$ meV.

at 10 and 65 K; separate peaks are no longer resolved at 300 K. Note that static stripe order is present at 10 K, but is absent at 65 and 300 K, where $T > T_{\text{st}}$. As observed previously,²⁹ the loss of stripe order results in a small decrease in the peak incommensurability and significant momentum-broadening of the scattered intensity.

In striking contrast, there is very little change in the high-energy scattering (41 and 95 meV) across T_{st} . By looking at the high-energy data, it is impossible to judge whether or not stripe-order is present. Admittedly, at 95 meV the shape of the magnetic scattering is limited by counting statistics; nevertheless, it is clear that there are no dramatic changes in the intensity or general \mathbf{Q} dependence of the magnetic signal. Even at 300 K, a temperature roughly six times the stripe-ordering temperature, the main effect at 41 meV seems to be relatively modest momentum broadening of the magnetic signal.

Another way to examine the thermal evolution of the magnetic correlations is through the density of states. Figure 2 shows $\chi''(\omega)$, the imaginary part of the spin susceptibility integrated over \mathbf{Q} in the antiferromagnetic

Brillouin zone. The biggest contribution to the error bars comes from uncertainties in subtracting background contributions. The attentive reader will note that the sharp spike at ~ 45 meV that was present in the previous results²⁸ is absent in the new results. We are now confident that this feature is due to a dispersive phonon, as it is also present³⁶ in isostructural $\text{La}_{1.67}\text{Sr}_{0.33}\text{NiO}_4$; we have taken better account of this phonon contribution in the current analysis. Background contributions including those from higher energy phonons ($\gtrsim 50$ meV) are also more carefully examined, and the resulting $\chi''(\omega)$ is slightly smaller than, but within error bars of that from previous analysis.

We have chosen to present $\chi''(\omega)$, rather than $S(\omega)$, because it more clearly illustrates the lack of dramatic changes with temperature. The lack of significant change is especially clear for $\hbar\omega > 30$ meV. Below 20 meV, we find an initial increase in $\chi''(\omega)$ on losing static stripe order, and then a return to lower values at 300 K. This behavior is somewhat different from that inferred from measurements of low-energy spin excitations with a triple-

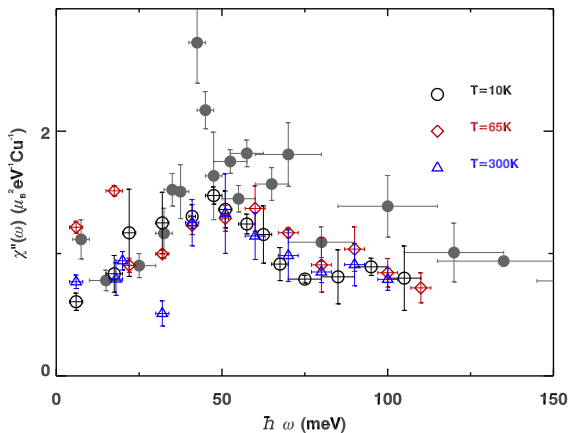


FIG. 2: (Color online) Imaginary part of the spin susceptibility, after \mathbf{Q} integration over the antiferromagnetic Brillouin zone, $\chi''(\omega)$ measured at $T=10$ K (black open circles), 65 K (red diamonds), and 300 K (blue triangles). The solid gray circles represent data from Ref. 28.

axis spectrometer.²⁹ There, fitting of a particular model cross section to the one-dimensional scans in \mathbf{Q} indicated that $\chi''(\omega)$ monotonically decreased with warming from the ordered state. The differences could possibly result from inadequacy of the model cross section or differing treatments of background, but we cannot rule out actual differences in the data.

The main point here is that over a substantial energy range there is little temperature dependence to $\chi''(\omega)$. Such behavior is what one typically finds in an ordered system, where the only impact of temperature is to change the occupancy of excited states. It is reminiscent of the variation of the scattering from the antiferromagnetically-correlated spins in La_2CuO_4 on warming through the Néel temperature.⁴¹ There, again, the loss of order is not readily detectable at higher excitations energies.

Returning to the \mathbf{Q} dependence of the data, one-dimensional constant- E cuts through \mathbf{Q}_{AF} , taken along [100] and [010] directions and averaged, are plotted in Fig. 3. (In the \mathbf{Q} direction perpendicular to each cut, data were averaged over a gaussian window with gaussian half-width, $\sigma_q = 0.02$ r.l.u.) We analyze each scan in terms of a symmetric pair of gaussian peaks split about \mathbf{Q}_{AF} and sitting on top of a weakly temperature-dependent background. At low temperature, the results are consistent with our previous observations.^{28,29} We can cleanly resolve incommensurate peaks in scans up to about 30 meV. At higher energies, the peaks move closer together, forming one broad peak that reaches a minimum width at ~ 54 meV. The scattering broadens and weakens at still higher energies.

With increasing temperature, the peak incommensurability (at low energies) is slightly reduced and the peak widths increase, consistent with previous work.²⁹ The in-

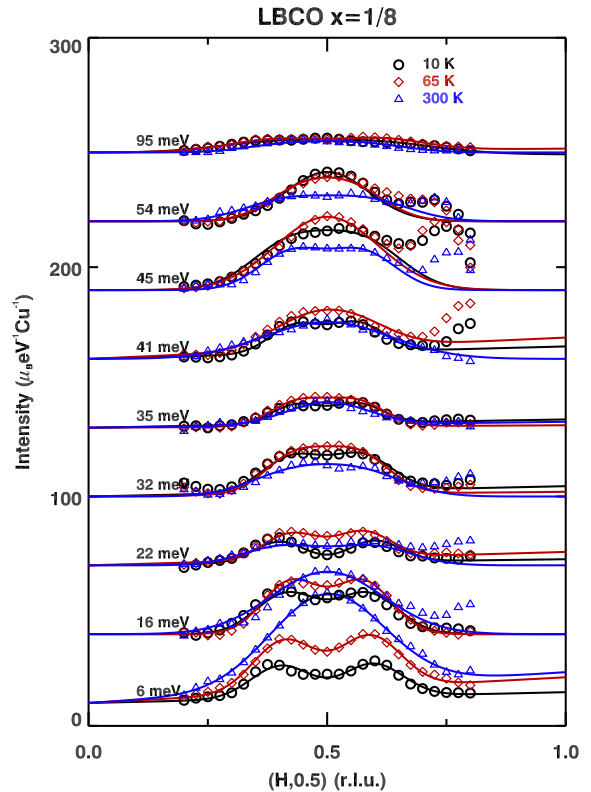


FIG. 3: (Color online) Linear intensity profiles measured through \mathbf{Q}_{AF} at different energy transfers. For each data set, we average linear cuts taken along [100] and [010] directions to improve statistics. The solid lines are fits to the data using two symmetric Gaussians displaced equally from $H = 0.5$, plus background. The peaks on the high- Q side (e.g., at $\hbar\omega = 16$ meV, 32 meV, 41 meV, and 45 meV) are due to phonon contributions.

crease in Q width indicates a decrease in the spin-spin correlation length.^{29,42} At 65 K, the incommensurability is less well resolved than in the ordered state, and no incommensurability can be detected for $T = 300$ K.

To summarize the energy and temperature dependence of the peak positions and widths, we have used the parameters obtained in the gaussian fits (indicated in Fig. 3) to create the contour plots shown in Fig. 4; here the peak intensity at each energy has been normalized to one. The solid lines indicate the effective dispersion characterizing our previous results²⁸ at 10 K. Qualitatively, the dispersion at $T = 10$ K (stripe-ordered phase) and at $T = 65$ K (disordered phase) are the same. At $T = 300$ K, while there is no incommensurability, the overall Q width is not greater than the spread in Q (due to incommensurability at low energies and upward dispersion at higher energies) at the lower temperatures.

The instantaneous spin-spin correlations are described by the equal-time spin correlation function,

$$S(\mathbf{Q}) = \int S(\mathbf{Q}, \omega) d\omega.$$

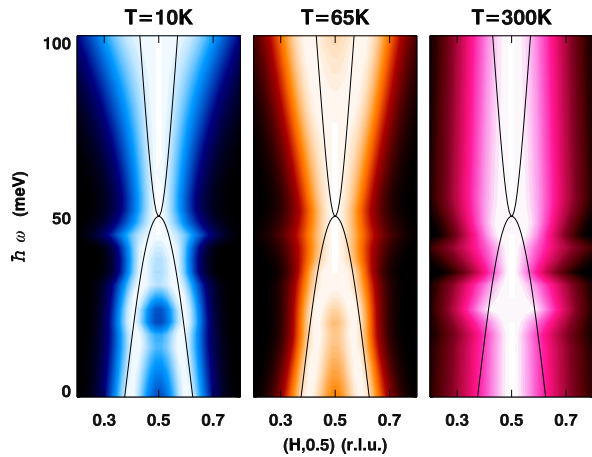


FIG. 4: (Color online) Two-dimensional maps plotted in energy-momentum space showing the fitted dispersions and Q widths at $T = 10$ K, 65 K, and 300 K. The signal is sliced along the $[100]$ direction in \mathbf{Q} , through \mathbf{Q}_{AF} . As a reference, the solid lines denote the dispersion at low temperature obtained in Ref. 28.

It is fairly clear from the data in Fig. 3 that, in the disordered phase, $S(\mathbf{Q})$ will be a broad peak centered at \mathbf{Q}_{AF} . We have used two methods to evaluate the integral. The first approach is to directly integrate the experimental $S(\mathbf{Q}, \omega)$ data. There are two drawbacks to this method. One is that the dominant signal is due to phonons (see Fig. 1 of Ref. 43); integration over energy should give some averaging over the phonon signals, but is not guaranteed to yield a smooth background. The second issue is the magnetic form factor, which varies with energy because Q_z , the component of \mathbf{Q} perpendicular to the CuO_2 planes, is a function of the energy transfer. In dividing the form factor out of the data, we also modify the phonon contributions whose \mathbf{Q} dependence we are hoping will largely cancel in the integral. This correction did not seem to have much impact on the nature of the net phonon background. The second method used is to integrate signal obtained from fits to the data, as shown in Fig. 3.

The results for $S(\mathbf{Q})$ are presented in Fig. 5. Panels (a)-(c) show the results obtained from direct integration of the data, after subtraction of a background proportional to Q^2 , at temperatures at 10 K, 65 K, and 300 K. One can see that the shape and size of the instantaneous structure factor does not change greatly with temperature. Cuts along $\mathbf{Q} = (H, 0, 0)$ are shown in Fig. 5(d). The symbols represent the direct integration over the data, while the lines correspond to the integration over the fitted magnetic signal. The difference in the results from the two approaches is due to the limited cancellation of phonon structures in the direct integration method. We believe that the integration over the fits provides a more reliable measure of $S(\mathbf{Q})$. We should also note that the result at 10 K is incomplete in that we

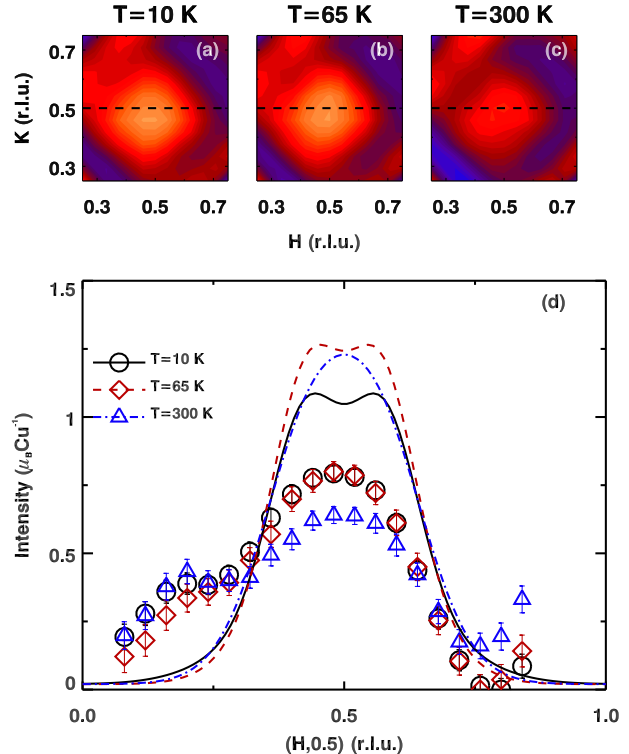


FIG. 5: (Color online) Measurements of $S(\mathbf{Q})$. (a), (b), and (c) show the energy integrals (over the interval 4 to 110 meV) of the $E_i = 140$ meV data, corrected for the magnetic form factor, at temperatures of 10 K, 65 K, and 300 K, respectively. A background varying as Q^2 has been subtracted in order to emphasize the magnetic response. The diagonal streaks near the upper left and lower right corners are artifacts due to spurious signals at the detector edges. (d) Cuts along the \mathbf{Q} path indicated by dashed lines in (a)-(c). Symbols represent the integral of over the data, while the lines correspond to integration over the fitted magnetic signal (from Fig. 3). The difference in the two approaches is due to the differing treatments of the phonon background.

have not included the sharp peaks from the elastic channel in the integration; although the relative weight in the elastic peaks is not large, their narrow Q widths would lead them to dominate the shape of $S(\mathbf{Q})$.

From Fig. 5(d), one can see that the width of $S(\mathbf{Q})$ shows virtually no change with temperature. Quantitatively, the half width is $\kappa = 0.15 \pm 0.02$ r.l.u. If we were to assume that the spin correlations fall off exponentially in real space, then we would obtain a correlation length of $\xi = 2\pi/\kappa a = 4.0 \pm 0.5$ Å, or approximately one Cu-Cu nearest-neighbor spacing. The values we obtain for κ and ξ are virtually the same as those reported by Hayden *et al.*⁴⁴ for LSCO $x = 0.14$ at 17 K; the magnitude of $S(\mathbf{Q})$ is also similar.

In considering the significance of κ and its lack of temperature dependence, it is worth noting that the shape of $S(\mathbf{Q})$ (at least that given by the lines in Fig. 5) is dif-

ferent from the lorentzian one would expect if the spatial correlations decayed exponentially. Instead, the shape is rather flat-topped. To see what may determine this shape, it is instructive to look back at Fig. 4. The limiting feature for the Q width seems to be the low-energy incommensurability that is resolvable at lower temperatures. That feature is determined by the facts that the antiferromagnetic correlations are constrained to narrow domains by the charge stripes and that the phase of the antiferromagnetic correlations must flip by π on crossing a charge stripe. Thus, the magnitude of κ , together with the large energy scale for the magnetic excitations, appear to reflect the spatial inhomogeneity of the spin and charge correlations.

IV. DISCUSSION

The present results show that the energy scale characterizing spin fluctuations in LBCO ($x = \frac{1}{8}$) is insensitive to the ordering of charge stripes. Given that the maximum in $\chi''(\omega)$ is at ~ 50 meV, it is not surprising that thermal energy alone has a modest impact on the spectrum, even at 300 K. What is more important is the observation that there is no qualitative change in the magnetic spectrum due to the loss of stripe order. This is another piece of evidence that the electronic and magnetic correlations in the stripe-ordered phase are similar to those in the disordered phase. It is consistent with the idea that the disordered state consists of a stripe liquid⁴⁵ or nematic phase.⁴⁶ Evidence for a stripe liquid phase has also been observed in layered nickelates⁴⁷; the difference in cuprates is that quantum fluctuations may prevent ordering, in the absence of a crystal symmetry that removes the degeneracy between equivalent stripe orientations.

That the electronic properties of the stripe-ordered state are subtly different from those in the disordered phase has been demonstrated by a couple of recent experiments. Angle-resolved photoemission and tunneling measurements³⁸ indicate a d-wave-like gap similar to that found in superconducting samples. The maximum amplitude of the gap is ~ 20 meV. The gap also appears in the in-plane optical conductivity,³⁷ where one sees evidence both for excitations across the gap and a collective mode. In the disordered phase, the in-plane optical conductivity looks essentially identical to that in LSCO and other superconducting cuprates of comparable hole content.

A picture of alternating doped and undoped two-leg ladders, with no ordered spins in the doped ladders, is consistent with the magnetic stripe order.²⁹ It was argued previously²⁸ that the effective magnetic dispersion observed in the stripe-ordered phase can be understood in terms of the excitations of the ordered spin ladders with a weak effective coupling across the doped ladders; the energy scale is set by the superexchange energy of the parent insulator (La_2CuO_4 in this case).^{23,27,28} Various model calculations of the excitation spectra have

been based on this picture.^{48,49,50,51,52} It should be noted, however, that this is certainly an over-simplified starting point for the spin dynamics, because it ignores the spin degrees of freedom in the doped stripes. Here we reconsider the nature of the dispersion.

Inelastic neutron scattering measurements on underdoped crystals of YBCO with varying degrees of twinning indicate that the magnetic excitations above the “resonance” energy seem to have an isotropic dispersion and intensity, in contrast to excitations at lower energies, which do show significant orientational anisotropy.^{20,53} These YBCO crystals do not exhibit any static stripe order; however, the dispersions do show strong similarities to those in LBCO,²⁷ and it seems sensible to look for a common understanding. From the similar characters, we infer that the magnetic excitations above 50 meV in LBCO likely close to 4-fold symmetric within each CuO_2 plane. Such behavior would be inconsistent with the over-simplified model,^{48,49,50,51,52} but could it be compatible with a more general stripe model?

To answer this question, we first need to consider the nature of spin excitations in doped two-leg ladders. One relevant model system is $\text{Sr}_{14}\text{Cu}_{24}\text{O}_{41}$, a compound containing both Cu-O chains and lightly hole-doped^{54,55,56} two-leg spin ladders. Neutron-scattering studies⁵⁷ of the response from the ladders provide evidence for gapped triplet excitations very similar to those in undoped ladders.⁵⁸ The survival of singlet correlations and triplet excitations in doped two-leg ladders is certainly expected theoretically,^{59,60} and the spin correlations in such systems are believed to be relevant to hole pairing.^{61,62}

Another result relevant to the problem of doping holes into a quantum spin system involves the Haldane-chain compound $\text{Y}_{2-x}\text{Ca}_x\text{BaNiO}_5$. For $x = 0$, the Ni-O chains behave as decoupled $S = 1$ spin chains, with a gap of approximately 9 meV for triplet excitations⁶³ and a dispersion extending to greater than 60 meV.⁶⁴ On doping holes into the chains, through Ca substitution for Y, there is no qualitative change in the dispersion of the triplet excitations; the biggest change is the appearance of new incommensurate excitations within the spin gap of the undoped system.⁶⁴

With these results in mind, let us return to the case of the stripe-ordered phase. The incommensurate magnetic peaks tell us that the nearest-neighbor antiferromagnetic domains must have an antiphase relationship.⁴⁰ The same correlation is relevant for all of the magnetic excitations at energies $\lesssim 50$ meV. This constraint no longer applies at higher energies. For $\hbar\omega \gtrsim 50$ meV, the correlated fluctuations of the moments in neighboring domains are essentially in phase, rather than out of phase—we have a dispersion of excitations from \mathbf{Q}_{AF} as in an antiferromagnet with a gap. If the gap corresponds to the the spin gap in the doped ladders, then we might expect the spin excitations of the doped ladders to contribute to the in-phase dispersion. The net dispersion could be fairly isotropic. (Note that a more isotropic

dispersion of high-energy excitations is obtained in the Gutzwiller-mean-field calculation of stripes by Seibold and Lorenzana,⁶⁵ where the assumptions of the spin-only models were not made.)

A plausible, phenomenological picture, then, is that the magnetic excitations above a spin gap energy [~ 50 meV in the case of LBCO ($x = 1/8$)] are similar to two-dimensional antiferromagnetic spin waves,²⁰ but with a very short correlation length. The impact of the doped holes becomes directly apparent at lower energies, where one observes a downward dispersion. From the evolution of the spin excitations in LBCO from the spin-ordered to the disordered phase, the lowest-energy incommensurate spin excitations must be the Goldstone modes of the stripe phase.

Returning to the possibility that a stripe-liquid character is common to the hole-doped cuprates, we note that objections have been raised in the case of YBCO. In particular, Bourges *et al.*⁶⁶ have pointed out that while a dispersion downward from the “resonance” energy is observed in $\text{YBa}_2\text{Cu}_3\text{O}_{6.85}$ for $T < T_c$, it disappears for $T \gtrsim T_c$. In considering this objection, it should first be noted that no measurements were presented for energies lower than 25 meV; presumably, the magnetic signal was too weak to analyze at lower energies. Next, consider our results for LBCO at 65 K in Fig. 3. No incommensurate features can be resolved at energies above ~ 30 meV; the incommensurability only becomes clear at lower energies. Thus, the absence of an obvious dispersive or incommensurate character at higher energies and temperatures is completely compatible with our observations in the stripe-liquid phase of LBCO. Another relevant observation in Figs. 3 and 5 is that the net Q width of the dominant magnetic signal associated with the stripe correlations does not change dramatically with temperature. Similarly, one observes the same net Q width in $\text{YBa}_2\text{Cu}_3\text{O}_{6.85}$ both above and below T_c .⁶⁶

In LBCO ($x = 1/8$), the most significant changes with temperature seem to be associated with the Q width, κ , and incommensurability of the low-energy excitations, as observed in a previous study.²⁹ In the LTO phase, κ decreases with cooling. This behavior is correlated with a decrease in the energy width of the Drude peak found in the optical conductivity.³⁷ Similarly, the absence of incommensurability in the low-energy magnetic excitations at room temperature is correlated with the disappearance of the Drude peak into a very broad mid-infrared

continuum. We infer that the development of electronic coherence in the copper-oxide planes is associated with the growth of stripe correlations on cooling.

Such trends extend well beyond LBCO. In optimally-doped LSCO, Aeppli *et al.*⁴² found that κ for low-energy incommensurate spin excitations shows quantum critical behavior, reflecting the evolution of stripe correlations with cooling, but with stripe order avoided due to quantum fluctuations. Optical conductivity studies of LSCO show a linear variation of the Drude energy width with temperature for a range of dopings.^{67,68} Thus, it appears that, rather than competing, stripe and “nodal-metal”⁶⁹ coherence develop synergistically. It is only static stripe order that competes with superconductivity, and even then, stripe order is compatible with gapless electronic excitations at the nodal points.^{37,38}

V. CONCLUSION

We have presented an inelastic neutron scattering study of magnetic excitations at energies up to 100 meV for LBCO ($x = 1/8$) at temperatures below and above the stripe ordering temperature. While the excitations at low energies are broadened in Q on warming, the magnetic signal for $\hbar\omega > k_B T$ shows remarkably little change. We interpret these results as evidence of a stripe-liquid phase for $T > T_{st}$. We have noted similarities between the magnetic excitation spectrum of the stripe-liquid phase and that seen in other cuprates. We have also pointed out that the coherence of the stripe-liquid correlations and low-energy charge excitations develop synergistically with cooling.

Acknowledgements

It is a pleasure to acknowledge helpful discussions with S. A. Kivelson and E. W. Carlson. Work at Brookhaven is supported by the U.S. Department of Energy’s Office of Science under Contract No. DE-AC02-98CH10886. Work at Tohoku University is supported by a Grant-in-Aid for Scientific Research from MEXT. This work has also benefited from the U.S.-Japan Cooperative Program on Neutron Scattering.

¹ M. A. Kastner, R. J. Birgeneau, G. Shirane, and Y. Endoh, *Rev. Mod. Phys.* **70**, 897 (1998).

² J. Orenstein and A. J. Millis, *Science* **288**, 468 (2000).

³ S. A. Kivelson, I. P. Bindloss, E. Fradkin, V. Oganesyan, J. M. Tranquada, A. Kapitulnik, and C. Howald, *Rev. Mod. Phys.* **75**, 1201 (2003).

⁴ J. Zaanen, O. Y. Osman, H. V. Kruis, Z. Nussinov, and J. Tworzydło, *Phil. Mag. B* **81**, 1485 (2001).

⁵ K. Machida, *Physica C* **158**, 192 (1989).

⁶ S. Sachdev and N. Read, *Int. J. Mod. Phys. B* **5**, 219 (1991).

⁷ J. Brinckmann and P. A. Lee, *Phys. Rev. Lett.* **82**, 2915 (1999).

⁸ Y.-J. Kao, Q. Si, and K. Levin, *Phys. Rev. B* **61**, R11898 (2000).

⁹ Y. Yamase and H. Kohno, *J. Phys. Soc. Japan* **70**, 2733

- (2001).
- ¹⁰ A. V. Chubukov, B. Jankó, and O. Tchernyshyov, *Phys. Rev. B* **63**, 180507R (2001).
 - ¹¹ F. Onufrieva and P. Pfeuty, *Phys. Rev. B* **65**, 054515 (2002).
 - ¹² T. E. Mason, A. Schröder, G. Aeppli, H. A. Mook, and S. M. Hayden, *Phys. Rev. Lett.* **77**, 1604 (1996).
 - ¹³ B. Lake, G. Aeppli, T. E. Mason, A. Schröder, D. F. McMorrow, K. Lefmann, M. Isshiki, M. Nohara, H. Takagi, and S. M. Hayden, *Nature* **400**, 43 (1999).
 - ¹⁴ J. M. Tranquada, C. H. Lee, K. Yamada, Y. S. Lee, L. P. Regnault, and H. M. Rønnow, *Phys. Rev. B* **69**, 174507 (2004).
 - ¹⁵ R. Gilardi, A. Hiess, N. Momono, M. Oda, M. Ido, and J. Mesot, *Europhys. Lett.* **66**, 840 (2004).
 - ¹⁶ N. B. Christensen, D. F. McMorrow, H. M. Rønnow, B. Lake, S. M. Hayden, G. Aeppli, T. G. Perring, M. Mangkorntong, M. Nohara, and H. Tagaki, *Phys. Rev. Lett.* **93**, 147002 (2004).
 - ¹⁷ B. Vignolle, S. M. Hayden, D. F. McMorrow, H. M. Rønnow, B. Lake, C. D. Frost, and T. G. Perring (2005), *cond-mat/0701151*.
 - ¹⁸ S. M. Hayden, H. A. Mook, P. Dai, T. G. Perring, and F. Doğan, *Nature* **429**, 531 (2004).
 - ¹⁹ D. Reznik, P. Bourges, L. Pintschovius, Y. Endoh, Y. Sidis, T. Matsui, and S. Tajima, *Phys. Rev. Lett.* **93**, 207003 (2004).
 - ²⁰ C. Stock, W. J. L. Buyers, R. A. Cowley, P. S. Clegg, R. Coldea, C. D. Frost, R. Liang, D. Peets, D. Bonn, W. N. Hardy, et al., *Phys. Rev. B* **71**, 024522 (2005).
 - ²¹ S. Pailhès, Y. Sidis, P. Bourges, V. Hinkov, A. Ivanov, C. Ulrich, L. P. Regnault, and B. Keimer, *Phys. Rev. Lett.* **93**, 167001 (2004).
 - ²² V. Hinkov, S. Pailhès, P. Bourges, Y. Sidis, A. Ivanov, A. Kulakov, C. T. Lin, D. P. Chen, C. Bernhard, and B. Keimer, *Nature* **430**, 650 (2004).
 - ²³ J. M. Tranquada, H. Woo, T. G. Perring, H. Goka, G. D. Gu, G. Xu, M. Fujita, and K. Yamada, *J. Phys. Chem. Solids* **67**, 511 (2006).
 - ²⁴ P. Bourges, in *The Gap Symmetry and Fluctuations in High Temperature Superconductors*, edited by J. Bok, G. Deutscher, D. Pavuna, and S. A. Wolf (Plenum, New York, 1998), p. 349.
 - ²⁵ P. Dai, H. A. Mook, R. D. Hunt, and F. Doğan, *Phys. Rev. B* **63**, 054525 (2001).
 - ²⁶ H. F. Fong, P. Bourges, Y. Sidis, L. P. Regnault, A. Ivanov, G. D. Gu, N. Koshizuka, and B. Keimer, *Nature* **398**, 588 (1999).
 - ²⁷ J. M. Tranquada, *cond-mat/0512115*.
 - ²⁸ J. M. Tranquada, H. Woo, T. G. Perring, H. Goka, G. D. Gu, G. Xu, M. Fujita, and K. Yamada, *Nature* **429**, 534 (2004).
 - ²⁹ M. Fujita, H. Goka, K. Yamada, J. M. Tranquada, and L. P. Regnault, *Phys. Rev. B* **70**, 104517 (2004).
 - ³⁰ P. Abbamonte, A. Rusydi, S. Smadici, G. D. Gu, G. A. Sawatzky, and D. L. Feng, *Nature Phys.* **1**, 155 (2005).
 - ³¹ M. Hücker and M. v. Zimmermann, (unpublished).
 - ³² M. Hücker, G. D. Gu, and J. M. Tranquada (2005), *cond-mat/0503417*.
 - ³³ A. T. Savici et al., *Phys. Rev. Lett.* **95**, 157001 (2005).
 - ³⁴ A. T. Boothroyd, D. Prabhakaran, P. G. Freeman, S. J. S. Lister, M. Enderle, A. Hiess, and J. Kulda, *Phys. Rev. B* **67**, 100407(R) (2003).
 - ³⁵ P. Bourges, Y. Sidis, M. Braden, K. Nakajima, and J. M. Tranquada, *Phys. Rev. Lett.* **90**, 147202 (2003).
 - ³⁶ H. Woo, A. T. Boothroyd, K. Nakajima, T. G. Perring, C. D. Frost, P. G. Freeman, D. Prabhakaran, K. Yamada, and J. M. Tranquada, *Phys. Rev. B* **72**, 064437 (2005).
 - ³⁷ C. C. Homes, S. V. Dordevic, G. D. Gu, Q. Li, T. Valla, and J. M. Tranquada, *Phys. Rev. Lett.* **96**, 257002 (2006).
 - ³⁸ T. Valla, A. V. Federov, J. Lee, J. C. Davis, and G. D. Gu, *Science* **314**, 1914 (2006).
 - ³⁹ S. Shamoto, M. Sato, J. M. Tranquada, B. J. Sternlieb, and G. Shirane, *Phys. Rev. B* **48**, 13817 (1993).
 - ⁴⁰ J. M. Tranquada, B. J. Sternlieb, J. D. Axe, Y. Nakamura, and S. Uchida, *Nature* **375**, 561 (1995).
 - ⁴¹ K. Yamada, K. Kakurai, Y. Endoh, T. R. Thurston, M. A. Kastner, R. J. Birgeneau, G. Shirane, Y. Hidaka, and T. Murakami, *Phys. Rev. B* **40**, 4557 (1989).
 - ⁴² G. Aeppli, T. E. Mason, S. M. Hayden, H. A. Mook, and J. Kulda, *Science* **278**, 1432 (1997).
 - ⁴³ S. Wakimoto, K. Yamada, J. M. Tranquada, C. D. Frost, R. J. Birgeneau, and H. Zhang (2006), *cond-mat/0609155*.
 - ⁴⁴ S. M. Hayden, G. Aeppli, H. A. Mook, T. G. Perring, T. E. Mason, S.-W. Cheong, and Z. Fisk, *Phys. Rev. Lett.* **76**, 1344 (1996).
 - ⁴⁵ J. Zaanen, M. L. Horbach, and W. van Saarloos, *Phys. Rev. B* **53**, 8671 (1996).
 - ⁴⁶ S. A. Kivelson, E. Fradkin, and V. J. Emery, *Nature* **393**, 550 (1998).
 - ⁴⁷ S.-H. Lee, J. M. Tranquada, K. Yamada, D. J. Buttrey, Q. Li, and S.-W. Cheong, *Phys. Rev. Lett.* **88**, 126401 (2002).
 - ⁴⁸ M. Vojta and T. Ulbricht, *Phys. Rev. Lett.* **93**, 127002 (2004).
 - ⁴⁹ G. S. Uhrig, K. P. Schmidt, and M. Grüninger, *Phys. Rev. Lett.* **93**, 267003 (2004).
 - ⁵⁰ M. Vojta, T. Vojta, and R. K. Kaul, *Phys. Rev. Lett.* **97**, 097001 (2006).
 - ⁵¹ D. X. Yao, E. W. Carlson, and D. K. Campbell, *Phys. Rev. Lett.* **97**, 017003 (2006).
 - ⁵² B. M. Andersen and O. F. Syljuåsen (2006), *cond-mat/0608251*.
 - ⁵³ V. Hinkov, P. Bourges, S. Pailhès, Y. Sidis, A. Ivanov, C. T. Lin, D. P. Chen, and B. Keimer (2006), *cond-mat/0601048*.
 - ⁵⁴ Y. Piskunov, D. Jérôme, P. Auban-Senzier, P. Wzietek, and A. Yakubovskiy, *Phys. Rev. B* **72**, 064512 (2005).
 - ⁵⁵ T. Vuletić, T. Ivek, B. Korin-Hamzić, S. Tomić, B. Gorschunov, M. Dressel, C. Hess, B. Büchner, and J. Akimitsu, *J. Phys. IV France* **131**, 299 (2005).
 - ⁵⁶ A. Rusydi, P. Abbamonte, M. Berciu, S. Smadici, H. Eisaki, Y. Fujimaki, S. Uchida, M. Rübhausen, and G. A. Sawatzky (2006), *cond-mat/0604101*.
 - ⁵⁷ C. Boullier, L. P. Regnault, J. E. Lorenzo, H. M. Rønnow, U. Ammerahl, G. Dhahlenne, and A. Revcolevschi, *Physica B* **350**, 40 (2004).
 - ⁵⁸ S. Notbohm, P. Ribeiro, B. Lake, D. A. Tennant, K. P. Schmidt, G. S. Uhrig, C. Hess, R. Klingeler, G. Behr, B. Büchner, et al., *Phys. Rev. Lett.* **98**, 027403 (2007).
 - ⁵⁹ G. Roux, S. R. White, D. Poilblanc, S. Capponi, and A. Läuchli, *Phys. Rev. B* **72**, 014523 (2005).
 - ⁶⁰ F. H. L. Essler and R. M. Konik (2006), *cond-mat/0607783*.
 - ⁶¹ E. Dagotto, J. Riera, and D. J. Scalapino, *Phys. Rev. B* **45**, 5744 (1992).
 - ⁶² S. A. Kivelson and E. Fradkin, *cond-mat/0507459*.
 - ⁶³ G. Xu, J. F. DiTusa, T. Ito, K. Oka, H. Takagi, C. Bro-

- holm, and G. Aeppli, Phys. Rev. B **54**, R6827 (1996).
- ⁶⁴ G. Xu, G. Aeppli, M. E. Bisher, C. Broholm, J. F. DiTusa, C. D. Frost, T. Ito, K. Oka, R. L. Paul, H. Takagi, et al., Science **289**, 419 (2000).
- ⁶⁵ G. Seibold and J. Lorenzana, Phys. Rev. Lett. **94**, 107006 (2005).
- ⁶⁶ P. Bourges, Y. Sidis, H. F. Fong, L. P. Regnault, J. Bossy, A. Ivanov, and B. Keimer, Science **288**, 1234 (2000).
- ⁶⁷ F. Gao, D. B. Romero, D. B. Tanner, J. Talvacchio, and M. G. Forrester, Phys. Rev. B **47**, 1036 (1993).
- ⁶⁸ J. Takeya, Y. Ando, S. Komiyama, and X. F. Sun, Phys. Rev. Lett. **88**, 077001 (2002).
- ⁶⁹ Y. S. Lee, K. Segawa, Z. Q. Li, W. J. Padilla, M. Dumm, S. V. Dordevic, C. C. Homes, Y. Ando, and D. N. Basov, Phys. Rev. B **72**, 054529 (2005).